High-Capacity Millimeter Wave Channel for 5G and Future Generation Systems Deployment in Tropical Region using NYUSIM Algorithm

Isaac O. Babarinde[1]* iD , Joseph S. Ojo[1] iD , Moses O. Ajewole[1] iD

[1]Department of Physics, School of Physical Science, Federal University of Technology Akure, Nigeria
Email: babarindeisaac2@gmail.com, ojojs_74@futa.edu.ng, oludare.ajewole@futa.edu.ng

* Corresponding author's e-mail address: babarindeisaac2@gmail.com

Abstract: Based on real-time field data from tropical outdoor microcellular networks (Akure, Nigeria), this study investigates the propagation of high-capacity millimeter waves (mmWave) in the 30-100 GHz frequency range. The data covers simultaneous measurements of rainfall rate and received signal strength (RSS) over a 300-meter path length between a Communication Research Lab (CRL) in FUTA Nigeria and the National Television Authority Tower at Iju Akure Nigeria at one-minute sampling time over a year (Jan 2021–Dec 2021). The study investigates the average network availability derived from the real-time data of rain rates. It compares the distributions of the measured rain-induced attenuation at various times of signal unavailability for 30 GHz with the modified anticipated attenuation by the Synthetic Storm Techniques (SST) model. Using MATLAB software and the most recent NYUSIM channel model software package (Version 3.1), an investigation of important propagation channel characteristics such as route loss, fade margin, and received power during heavy rains was also conducted. Based on convective and stratiform rain types, the focus on the propagation characteristics of a typical network provider, a Mobile Telecommunication Network (MTN), was assessed power obtained at the receiving end, signal loss along the route, and the interval of signal fading. The results show that the modified SST model provides high consistency with the measured attenuation through the outdoor links. The signal loss of about 80 dB is needed to be compensated as the rain rates approach 140 mm/hr over the 300-meter path length. The study also demonstrates that for multidirectional and oriented directional antenna links, regardless of the fading due to rain, the NYUSIM platform model provides a better representation of the power delay profile. The research outcome will provide useful information for setting up fifth-generation (5G) and other future wireless networks for outdoor applications, especially in tropical areas.

Keywords: Large Scale parameters, Millimeter-wave, NYUSIM channel model, Wireless Network, 5G

1. INTRODUCTION

The wireless communication industry has undergone remarkable growth in recent years, and certain technological advancements have led to the development of large numbers of gadgets that utilize the wireless communication procedure for their signal reception and transmission. Carrier frequency bands are necessary for the propagation of wireless signals from sender to receiver [1]. The current state of technology, which uses

commonly utilized frequency-modulated devices like the microwave, is vulnerable to significant damage as the number of consumers increases. The availability of limited bandwidth for sharing at these lower frequency bands leads to the depletion of propagated signals [2]. The rapid increase in the amount of data being transferred has rendered lower frequency bands insufficient for current and future generations of wireless networks [3]. There is a limited amount of spectrum that is currently accessible to cellular networks. As a result, different methods are employed to boost spectral efficiency [4]. These methods include interference coordination, multiple inputs and multiple outputs (MIMO), efficient channel coding, and orthogonal frequency division multiplexing (OFDM) [5]. However, a single increase in spectral efficiency is insufficient to provide high user data rates. As a result, considerably higher frequency bands like the millimeter wave band, which has frequencies between 30 and 300 GHz, need to be the focus of the research. This frequency band is known as the millimeter wave band (mmWave) because the wavelength varies from 1 to 10 mm [6]. A promising technology for cellular systems in the future is mmWave [4]. The use of mmWave has emerged as a significant technological breakthrough for various wireless mobile technologies, such as fifth-generation (5G), sixth-generation (6G), and other upcoming ones. However, its implementation has also introduced a few impediments to the current networks [7]. Hence, research attention needs to focus on qualitative studies for absolute optimization of the propagation characteristics of each environment for accurate deployment of the new mobile network using the mmWave [8]. Propagating signals in the mmWave band are highly susceptible to distortion, and different factors tend to militate against successful propagation. One of which includes the metrological properties of the surrounding environments like rain, haze, fog, and humidity. Among the hydrometeors, rain plays a vital role in achieving good-quality signals.

The rain, a prominent obstacle to propagation at the mmWave and other higher frequency bands, varies from region to region. The impact is considerably more significant in tropical regions, where there is a greater incidence of heavy rain with huge raindrop sizes [9]. The size distribution of raindrops varies according to geographic location, and they can approach the size of a radio wave in mm [10]. Therefore, as mmWave signals have similar sizes to raindrops, they are more susceptible to being blocked by them than signals with longer wavelengths [11]. This may significantly impact mmWave signal transmission and result in severe signal attenuation loss. As the rain increases in magnitude, frequency, and density, the degree of attenuation due to rain (ADR) also quickly rises [7]. Therefore, the rain fade effect is one of the main obstacles to mmWave propagation in the new mobile network system [8]. Rain can absorb, scatter, depolarize, and diffract signals from millimeter waves. This could prevent it from spreading, leading to a significant loss in signal strength over the actual propagation channel length [12]. When the air is not clear, atmospheric absorption and rain attenuation increase path loss and reduce communication range [13]. Therefore, a major challenge to the installation of future generations of mobile networks is the substantial rain attenuation of the mmWave band in tropical areas [14]. Utilizing channel simulators and computer-aided design tools is essential for accurately modelling and creating propagation channel behaviors because there is no universal channel model that correctly performs in all deployment scenarios across a variety of environments [2]. This research aims to significantly contribute to the field of high-capacity wireless deployments as one of the few studies to concentrate on mmWave communication channels, particularly in the tropical region of Nigeria. The impact of rain over the implementation of the new generation of networks like 5G and 6G in terms of its effect on the received signal power and the resultant fade margin were visualized across different transmission frequencies representing the mmWave band (30–100 GHz) using the New-York University Simulator (NYUSIM) [3]. In enhancing the current literature, our simulation encompassed a broad spectrum of frequencies, as well as two distinct levels of network availability: 99.9% and 99.99%. These considerations specifically addressed the impact of rain rate in the simulated scenarios. Utilizing the NYUSIM algorithm and leveraging real-world measurement data for the urban microcell (UMi) scenario, a model was created to analyze the impact of rain on a line-of-sight (LOS) mmWave transmission link operating in the 30-300 GHz frequency range over a path length of 300 km. The study focused on analyzing the effect of a minute sampling of rain rate on the fade margin (FM) and the mmWave link availability. The efficiency of the proposed channel was evaluated, and the NYUSIM simulator was used to characterize the effects of rain on the essential channel features of tropical climates. By incorporating rain attenuation into all time-varying envelopes of the multipath components in the channel impulse response (CIR) of the received signal, the simulator successfully characterized the influence of rain [3]. Several studies have been conducted on the 5G channel model, especially in the temperate region. Among these studies is the work of [15], who reported 5G link platforms for frequency bands up to 100 GHz using a ray tracing approach for specific bands between 6 and 100 GHz based on field data. The research employed a 3D-channel model that covers common scenarios for urban macrocells (UMa) and microcells (UMi) in cities. Ref. [16] conducted a study comparing the network routing parameters for the 73 GHz and 28

GHz frequency spectrums with the currently used 2.14 GHz frequency spectrum for LTE-A. The researchers employed the Alpha-Beta-Gamma (ABG) path loss model and varied user count in the cell to estimate several performance parameters using a Matlab-platform Vienna LTE-A system-level generator, including mean-user, peak-user, and mean cell throughput, spectrum efficiency, and fairness index. It can be deduced that the mmWave frequency band improved the network's overall performance, resulting in higher spectrum efficiency compared to the 2.14 GHz frequency band. Additionally, a study by [17] examined the budget evaluation for a connection, outside propagation coverage, signal loss due to the route, and mmWave frequencies greater than 6 GHz. The study employed an oriented horn antenna at the base station and multi-directional antennas at the receiving end. It also measured the delay period of the links and the signal loss due to the path for different antenna orientations and frequencies in real-time settings. The results indicated that the unobstructed Line of Sight (LOS) channels at the selected frequencies of 28, 38, and 60 GHz obeyed the loss due to propagation-free space. However, for the obstructed line of sight (termed Non-LOS or NLOS), routes had notable delay spreads over different paths and necessitated the use of a wide range of pointing angles to establish propagation links. [10] emphasized the importance of maintaining hop length and availability for communication links through thorough planning and monitoring of 5G propagation links. The use of adaptive modulation and autonomous power regulation in conjunction with shorter hop lengths can result in a rise in the capacity for shorter radio links. Optimizing the network and topology can also reduce the average length of radio access lines, increasing network capacity overall. [18] also used the NYUSIM spatial consistency channel model for moving users and the ordinary model without spatial consistency for the static user at the 73 GHz millimeter waveband to itemize different channel parameters for performance verification in the LOS and NLOS environments. Simulation results show higher received signal power while spatial consistency is utilized for both the LOS and the NLOS compared with an ordinary model without spatial consistency in the UMi scenario. [19] recently used the NYUSIM model to investigate the channel diversity in the mmWave band by using the frequency bands 28, 38, and 78 GHz and analyzing the influence of spatial consistency parameters. Several situations of spatial consistency were examined by changing parameters such as path loss, received power, and path loss exponent in order to quantify the Power Delay Profile (PDP) in the UMi environment. The results showed several distinctive effects on the 5G mmWave channel characteristics. Similarly, [20] compared directional and omnidirectional propagation, the effects of the hottest and coldest months on propagation in a tropical area, and looked at large-scale mmWave properties, including delay spread loss due to path and the delay profile arising from power for both LOS and NLOS situations. In the study, various channel characteristics, such as received signal quality and temperature variations for each NLOS and LOS scenario, were noted. In this study, the NYUSIM channel simulator has been used to examine the influence of rain types on signal propagation across the 30-100 GHz frequency band for the deployment of 5G and other future wireless networks in a tropical region of Nigeria.

1.1 The NYUSIM channel model

The New York University (NYU) wireless team developed the Statistical Spatial Channel Model (SSCM) called NYU Simulator (NYUSIM). It has been considered a valid channel model [8]. Simulating physical mmWave outdoor channels falls under the category of stochastic spatial channel models [21]. The frequency range for this mm-wave-based channel model ranges from 0.5 to 100 GHz. The improved model creates sample functions of the directional and omnidirectional channel impulse response (CIR) [3]. The simulator has two operational modes: drop-based and spatial consistency. Channel impulse responses (CIRs) can be produced by NYUSIM, which runs Monte Carlo simulations at particular transmitter-to-receiver separation distances. Users can input both the number of samples and the range of transmitter-to-receiver separation distances. Figure 1 presents a typical graphical user interface for NYUSIM.
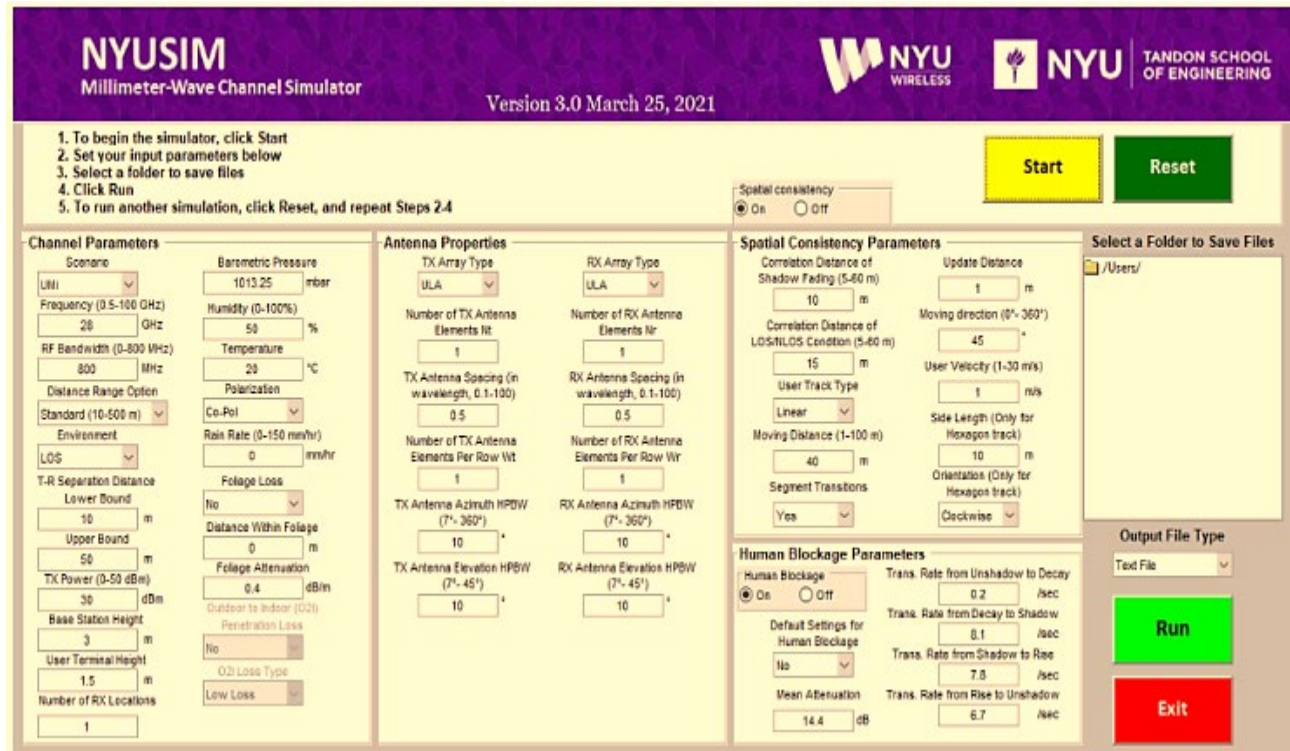
Figure 1. Graphical User Interface for NYUSIM

According to Fig. 1, for both channel and antenna configurations, the NYUSIM channel simulator needs 28 parameters. Twelve input parameters are provided for transmitter and reception antenna arrays in the GUI's panel antenna characteristics, but other input parameters are required for the propagation channel, which is included in the panel channel characteristics [3]. A brief description of some of the Large-scale parameters necessary for successful propagation in the mmWave band is presented in the following subsections:

1.1.1 Profile of the signal delay due to power

According to [22], the profile of the power delay (henceforth termed the PDP) depicts the mean power specified for particular delays during a signal. The profile is used to obtain the Root Mean Square (RMS) setback distributions and to identify the parameters associated with the multipath that exceed the noise peak based on their delays [23]. In situations with a line of sight (LOS), where 5G signals travel through mmWave channels, the PDP becomes a useful tool in examining path loss impacts. This is attributed to the fact that it accurately captures the physical attributes of the first multipath parameter of the delay (least delay). [24] highlights the ability of PDP to provide useful information on the path loss of 5G signals.

1.1.2 Path loss

Path loss (PL) is a crucial input variable for wireless communication channel models, as it illustrates the route of communication between the base station (transmitter-Tx) and end users (receiver-Rx). It considers factors like the separation distance between the Tx and Rx, environmental conditions, the frequency of the station, and the transmission environment [33]. Path loss (PL) is a crucial metric that indicates the average difference between the transmitting and receiving signal powers. It is widely employed in various applications such as link budget, system coverage, and interference analysis, as well as determining the signal-to-noise ratio (SNR) of cellular systems [3]. The CI-PL model is considered superior to other models since it is simpler and more precise. The multi-directional and oriented losses due to path models are developed based on the close-in model. Additionally, the NYUSIM route model is an advanced model that takes into account other atmospheric and weather conditions, resulting in a more accurate simulation of the channel [10]:

$$\text{Path loss } (f, d)[\text{dB}] = FSL(\text{f},d_o)[\text{dB}] + 10 \, nlog_{10}(\frac{d}{d_o}) + \text{A}_\text{T} [\text{dB}] + \chi\sigma^{CL} \tag{1}$$

$$FSL\ [dB] = 32.4[dB] + 20\ log_{10}(f) + 20log\ (d) \tag{2}$$

the parameter d_o is assumed to be 1 m in the NYUSIM model, FSL (f, d_0) in dB represents the signal strength at a typical distance in free space at a specified frequency (f), the losses due to the path in exponential form (PLE) are denoted by *n*, *d* is the separation distance between the Tx and Rx as measured in meters, where d ≥ d_0, the zero-mean Gaussian random variable with a standard deviation in dB is denoted as $\chi\sigma^{CL}$ denotes, and atmospheric attenuation is denoted by A_T.

1.1.3 Received Power

Friis's formula provides a way to analytically calculate the required power at the receiving antenna in a line-of-sight (LOS) mmWave point-to-point link using the following equation [10]

$$P_{RX}U\ [dBm] = P_{TX}\ [dBm] + G_{RX}a\ [dBi] +\ G_{TX}a\ [dBi]– FSL\ (f, d)\ [dB] \tag{3}$$

where the signal received at an unfaded level is denoted as and is the combination of free space path loss (FSL), the Tx power, and antenna gain, as stipulated by Friis' formula. The fade margin (FM) takes into consideration the detrimental factors that may impair the availability of the mmWave link, including atmospheric attenuation from weather events such as dust, snow, rain, fog, interference, and diffraction. It serves as the maximum allowable distortion [25]. However, if the attenuation exceeds the link margin, it can significantly jeopardize the physical layer's reliability, leading to a failed or disrupted connection [26]. Consequently, sufficient attention must be paid to link design, encompassing rainfall-induced attenuation, propagation characteristics, and information on multipath conditions, to ensure dependable radio connections and maximize availability [27].

1.1.4 Fade Margin

In this study, the Fade Margin (FM) is represented as the disparity between the strength of the unfaded received signal and the sensitivity of the receiver, and defined as:

$$FM\ [dB] = P_{RX}U\ [dBm] - P_{RX}th\ [dBm] \tag{4}$$

where $P_{RX}U$ [dBm] represents the received signal power, and P_{RX}th [dBm] represents the receiver's sensitivity threshold.

2.   EXPERIMENTAL MEASUREMENT

The research study location is Akure, Nigeria. Akure City is situated in the tropical, forested region of Nigeria and is the capital of Ondo State. It is located between 7.25°N and 5.19°E at an elevation of 358 meters above sea level. Its rainfall patterns are significantly influenced by the Atlantic Ocean and dry northwest winds originating from the Sahara Desert.

The southwest monsoon winds have an impact on this rain-producing region, which is distinguished by hot and humid areas [28]. Since the city is located in the tropics, it has two distinct seasons: wet (April to October) and dry (the rest of the year) [28]. The measurements of rain intensity and the level of the received signal (LRS) have been concurrently monitored for a year (January to December 2021) at 1-minute time intervals. The Tx and Rx equipment were positioned in between the FUTA Physics Department and an IJU communication tower, which is a 300-m short-path link with horizontal polarization at 30 GHz. 30 GHz has been considered because of its applicability and replicability based on the mm-wave platform. The obtained data (rain rate and RSL) were periodically measured and logged for every minute during rainy events. The experimental radio route was not blocked by any obstacles during the measurements, which were carried out at a normal LOS height of about 18 m. The experimental system setup is depicted in Figure 2. The information on the link is presented in Table 1. The rain rate was collected through the automatic weather station (AWS), which typically contains a rain gauge that measures the amount of rain that has fallen over time. The rain gauge utilized had a 200 mm diameter, and each of the tips of rainfall was calibrated to approximately 0.05 cm. The equipment's margin of error is around 6.8% for any rain rate exceeding 5 mm/h. The AWS data logger recorded measurements every 10 seconds, and integration took place at one-minute intervals. The rain gauge was

available for approximately 98.6% of the measurement period, with the remaining 1.4% reserved for equipment maintenance. The AWS data was filtered to extract the 1-minute integration time rain rate, and around 154 rainy events were recorded during the study period. Raw rain attenuation data was processed using MATLAB software, with the attenuation values averaged over a continuous 60-second time period.
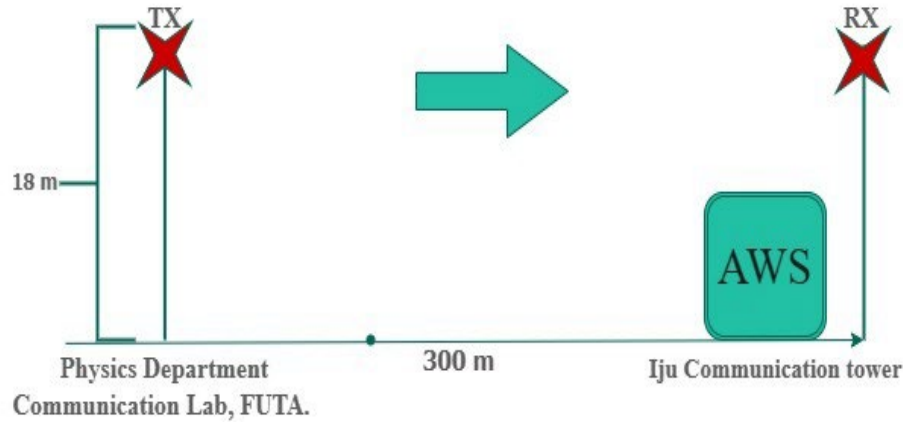
Figure 2. Experimental setup

A similarly programmed power meter was also installed at the receiver's end to measure the received power. The power meters were used to measure the signal's power before and after it traveled through the transmission medium. Using MATLAB software, the received power, expressed in dBμV, is quickly transformed to the equivalent RSS. The attenuation was calculated using the difference between the two measurements, i.e the RSL and transmission power from the experimental link as:

$$\text{Attenuation (dB)} = \text{transmitted power (dBm)} - \text{RSL (dBm)} \tag{5}$$

The signal quality was measured using a spectrum analyzer to obtain the power spectral density of the received signal over a range of frequencies. This allowed for the analysis of the quality of the received signal and the determination of the level of interference caused by ADR.

Table 1. Summary of the experimental link parameters

Link physical parameters	Specifications
Frequency band (GHz)	30 - 100
Antenna type	Directional
Link length (m)	300
Max Tx Power (dBm)	46.02
Tx-Rx height (m)	35
Polarization	Horizontal Polarization
Antenna Gain (dBi)	10

2.1 The Synthetic Storm Technique (SST) As Rain Attenuation Prediction Method for Mm-Wave

The rain attenuation was also simulated based on the synthetic storm techniques (SST) and compared with the measured ADR at 30 GHz. The SST at 30 GHz was used to extract the comparable real-time rain attenuation from the 1-year rain rate time series. The SST has been demonstrated to be the most effective at deriving rain attenuation from rain rate data. This is because of its capacity to accurately simulate a wide range of rainfall events and construct a realistic rain field using rain rate readings. This technique assumes that the rain rate at any given time can be modelled by the sum of several independent storms, each having a characteristic shape [26]. Synthetic storm methodologies enable the study of rain attenuation in various contexts and provide a

unique time series ADR. Additionally, SST can be used to evaluate rain attenuation at different radio frequencies, allowing for a more accurate determination of rain attenuation for different applications. The signal attenuation due to the effect of rain along the transmission path can be deduced using the synthetic storm technique (SST) model as presented in equation [5]:

$$A(t) = K_A R^{\alpha_A}(t) L_A + r^{\alpha_B} K_B R^{\alpha_B}(t) \left(L_A - L_B \right) \tag{6}$$

where R is the rain rate, the frequency-based parameters are denoted as k and α which are differently estimated for the layer specified for rain (A) and the layer specified for melting (B), respectively, L_A and L_B are radio path lengths [29].

3. RESULTS AND DISCUSSION

Results of the analysis generated from the measurement and the modelling are presented in this section.

3.1 Results on Rain Rate and Rain-Induced Attenuation from The Measurement and Modeling

Using the average measured 1-minute sampling rain rate and ITU region-based predicted value, Figure 3 displays the cumulative distribution function (CDF) based on a year data. The results indicate a rise in value of about 140 mm/h for the measured data, compared to the ITU's prediction of 120 mm/h for Akure. As also shown in Figure 3, the measured rainfall rate shows higher conformity with the ITU-R recommendation for time percentages higher than 0.1% and at 0.01% unavailability of time. However, deviation occurs at time percentages between 0.3% and 0.03% of the time. This implies the need to modify the ITU rain rate model for the region.

The impact of rain on signal propagation was measured using a signal generator and a power meter. At a predetermined frequency of 30 GHz, the signal generator generated a predetermined signal that was communicated from the Tx-Rx via the air medium. Figure 4 illustrates that on a typical rainy day, the range of the raw received signal level (in dBμV) falls between 27 dBμV and 68 dBμV at rainfall rates ranging from 0.5 mm/hr to 28 mm/hr, respectively. As the rainfall rate increases, the received signal power level experiences deep distortion. Therefore, as the rain intensity increases, the received signal undergoes continuous distortion, which can reach as high as 120 dB in extreme cases of heavy rainfall (although not shown here). The CDF of the observed ADR at 30 GHz over a path length of 300 m at various percentages of time (0.001% ≤ P ≤ 10%) is shown in Figure 5 for the experimental link.

The study's simultaneous rain rate and ADR observations allowed for statistically determining both parameters from equal probability values. As shown in Figure 6, the ADR at 30 GHz across a 300-m channel path was plotted against the one-minute rain rate determined by the rain gauge. The findings showed that changes in rain rate had a direct impact on attenuation levels. In particular, it was found that the signal loss over the 300-m path length was roughly 18 dB at a rain rate of 40 mm/h but reached 80 dB at a rain rate of 140 mm/h. A rain rate of 40 mm/h was present for 0.1% of the total network unavailability, and the study also found that the mean rain rate of 140 mm/h occurred at 0.01% unavailability of the time signal exceeded. These percentages are crucial, as they represent the major sub-categories of ideally affordable network outages for wireless networks that utilize the mm-wave band for propagation.
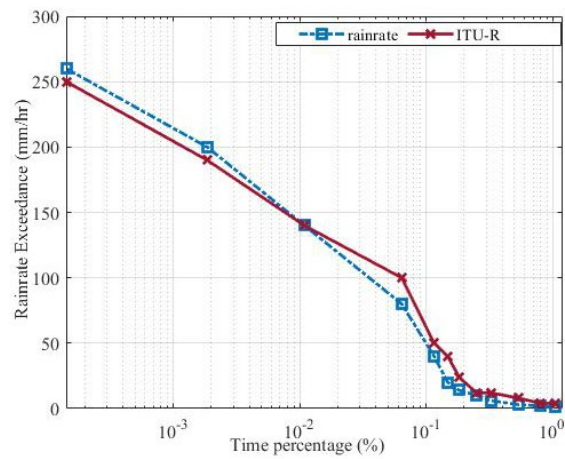
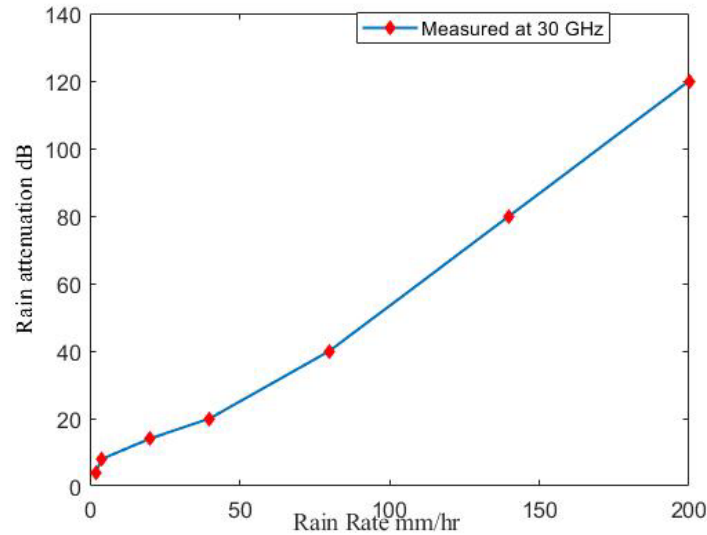**Figure 3**. Distribution of the measured rain rate cumulatively
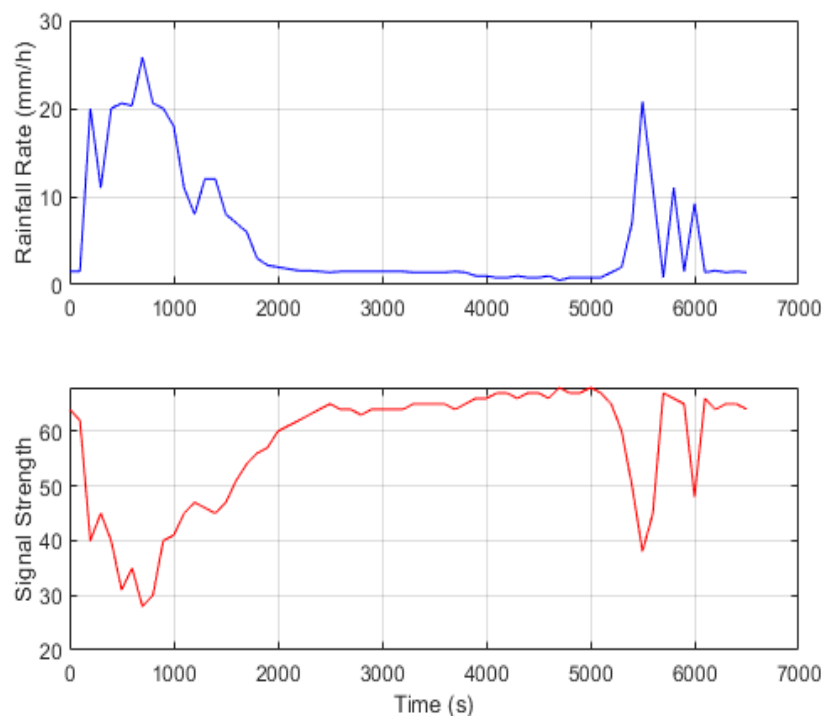
Figure 4. Influence of rain on the signal propagation over the experimental link
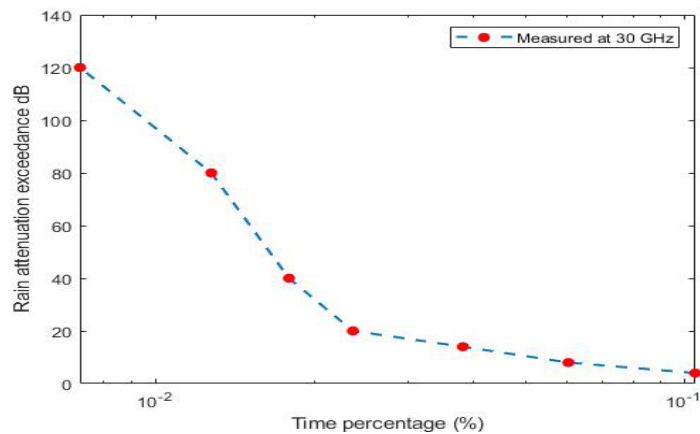

**Figure 5.** CDF measured ADR spread at 300 m link

Figure 6. Cumulative measured rain rate and ADR distribution at 30 GHz over 300 m.

Figure 7 compares the measured and anticipated ADR at 30 GHz across a link path of 300 m for various time percentages (0.001% ≤ P ≤ 10%). The Figure illustrates the predicted ADR exceedance values along with the measured values. It is observed that the predicted ADR values closely match the measured values, with a slight discrepancy of around 5% between the two. This indicates that the predicted ADR values are slightly higher than the measured values. For instance, at link unavailability of $R_{0.01}$, the measured ADR is 20 dB, whereas the predicted ADR is 23 dB. Several factors may contribute to this discrepancy, such as limitations in the prediction model, measurement errors, or changes in the environment. However, despite this discrepancy, the predicted ADR values can still provide a useful estimate of the actual ADR, especially when accurate experimental measurements are not available. It is essential that further analysis and investigation may be necessary to identify the cause of the discrepancy and improve the accuracy of the prediction model. However, the results from Figure 7 suggest that the model can be a valuable tool for estimating attenuation with minimal error. The predicted and measured attenuation exceedance in Figure 6 was compared at a frequency of 30 GHz. However, the SST method is frequency-independent, which means that it can be used to predict the attenuation of electromagnetic waves at any frequency even at 60 and 100 GHz.

Moreover, the SST technique has been validated for a significant range of frequencies, including 60 and 100 GHz [30], and has been found to provide accurate predictions of attenuation under different atmospheric conditions [30]. Figure 8 presents the attenuation generated using SST at frequencies between 60 and 100 GHz.
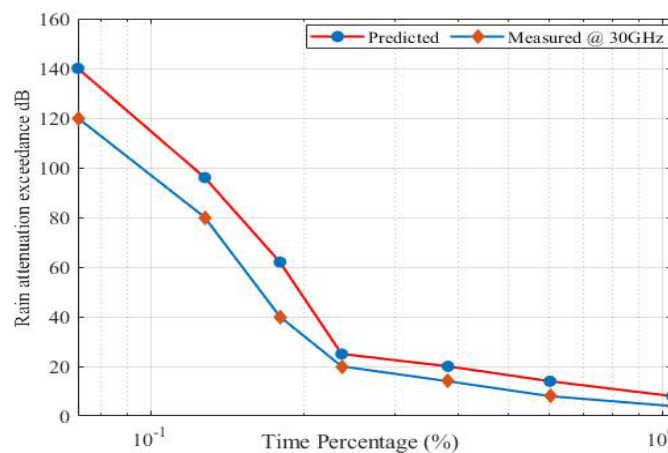
Figure 7. Measured and predicted cumulative ADR distribution at 300 m link
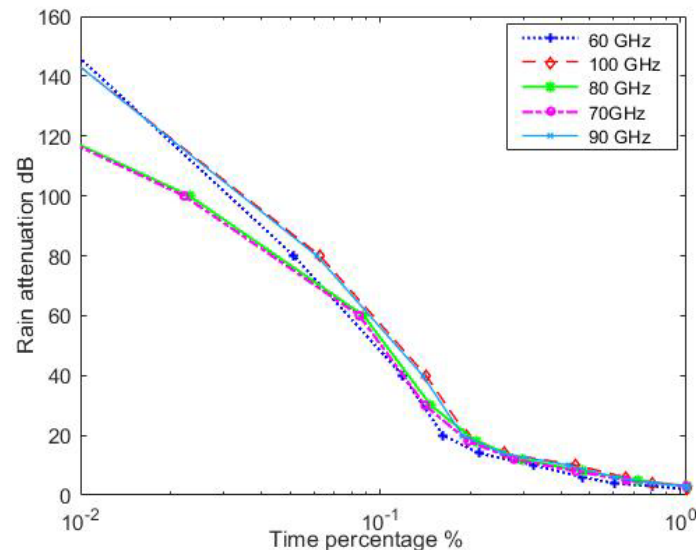
Figure 8. Cumulative distribution for the predicted rain attenuation at 60 and 100 GHz

Figure 8 further validates the higher susceptibility to attenuation due to atmospheric conditions such as rain, compared to lower-frequency bands. This can be attributed to the shorter wavelength of mmWave, which makes them more susceptible to scattering, absorption, and attenuation, by atmospheric conditions [1]. As a result, the attenuation through the SST is expected to be relatively high for both 60 and 100 GHz, with little difference in the trend as observed. In addition to the atmospheric attenuation due to rainfall, there is also the effect of atmospheric attenuation due to oxygen absorption, which is significant at frequencies above 60 GHz. Oxygen molecules in the atmosphere strongly absorb electromagnetic energy in the frequency range of 60-100 GHz, resulting in additional attenuation of signals at these frequencies [7]. This additional attenuation due to oxygen absorption at such frequencies makes the attenuation to be higher than at 100 GHz.

3.2 Profile of Signal Delay due to Power Based on the Propagation Parameters of a Network Provider Within Akure, Nigeria

A channel model has also been developed for analyzing wireless channels based on the propagation parameters of a mobile network provider (MTN) in the study region. To assess the further performance of mmWave communication networks, the simulation considered frequency ranges from 30 to 100 GHz. The resulting power delay profiles (PDPs) extracted at 30, 60, and 100 GHz are presented in Figures 9–14. The analysis focused on key channel information, such as the losses due to path length, power received, and fade margin, to predict the best frequency band within the mm-wave spectrum for tropical locations. Table 2 illustrates the setup of simulations and input parameters. The power delay profile of the channel, which characterizes the channel's time-varying response to transmitted signals, was generated using NYUSIM software version 3.1. The simulations were conducted for a cell size of 300 m in UMi/LOS outdoor situations for both multi-directional and oriented transmission scenarios. The resulting data was then used to assess the effects of the channel parameters on mm-wave channels.

Table 2. Configuration parameters for the NYUSIM simulations**.**

Channel parameters	Value(s)
Operational Frequency (GHz)	30-100 (at 5 GHz intervals)
Bandwidth due to RF (MHz)	800
Operating condition	Urban microcell (UMi)
Separation distance (m)	300
Transmit Power in dBm	46.02
Height of the base station (m)	35
Terminal height of the user (m)	1.5
Barometric Pressure in mbar	1012
Humidity in %	76.8
The temperature (℃)	27.1
Polarization	Co-Pol
Rain rate (mm/hr)	140,40
Tx and Rx Antenna Gain (dBi)	24
Tx antenna elements	1
Rx antenna elements	1

The following are the categories into which the analysis's findings have been divided:

3.3 The Influence of Antenna Variation

For both oriented and multi-directional antenna broadcasts of 24.6 dBi power gain and beam widths of 10, with a transmitting power of 46.02 dBm, the influence of the type of antenna on the mm-wave propagation route has been investigated. Figures (9–14) generally illustrate how directional antennas can effectively mitigate delay spread and minimize path loss encountered during transmission by directing the antenna beams at the correct angle, resulting in the concentration and directionality of the beam in a specific radiating direction. Also, the omnidirectional transmission causes a considerable delay spread that is closely dependent on the level of ADR caused by the type of rain that was predominant during the signal propagation. The observed difference is an average of about 15 ns throughout each of the selected frequencies. The primary source of this in LOS and NLOS scenarios is multipath components brought on by various scattering and reflection mechanisms. As a result, fewer, stronger signals from a few reliable multipath components will eventually reach the receiver. It is also clear that the directional antenna significantly reduces RMS delay while significantly increasing received power, path loss, and path loss exponent. Considering a typical scenario of stratiform rain type at 30 GHz, as shown in Figure 9a, the large-scale losses due to the path length for oriented and PDP, accounting for the ADR, are approximately 127.8 dB, with an expected path loss of 2.7. In this situation, if the transmission occurs in a LOS environment, the signal experiences an attenuation of more than 21.1 dB while propagating through the precipitation. Conversely, the path loss for the omnidirectional PDP is about 121.2 dB, and in LOS, the signal faces a dampening of merely 3.9 dB when transmitting through the rain, as shown in Figure 9b. Furthermore, the PLE in this scenario for the directional and omnidirectional profiles is 2.7 and 2.4, respectively (Figures 9a and 9b). This demonstrates how directed mm-wave solutions can enhance system performance. Compared to the omnidirectional channel, the directional channel results in higher losses. Yet, the received power increases when a directional antenna is employed since the majority of scattering and reflections occur outside the beam width of the antenna (Figures 9 and 10).

3.4 Influence of Different Rain Types

This study critically examines the influence of rainfall on mm-wave communication systems. As earlier stated, the region of study is characterized by two types of rainfall: stratiform and convective. Stratiform rainfall is a relatively steady, low-intensity type of rainfall that occurs over a relatively large area and typically lasts for an extended period, with a peak possible rate of around 20–50 mm/hr. Hence, the rain rate of 40 mm/hr stated earlier for the 0.1% of a network outage is used to depict the stratiform rain type for the purpose of simulation.

Convective rainfall, on the other hand, is a highly localized, intense type of rainfall that occurs over a smaller area and can have a high intensity, with a maximum possible rate of 100–200 mm/hr. Hence, the rain rate of 140 mm/hr stated earlier for 0.01 % of a network outage is used to depict the convective rain type for the purpose of simulation. Convective rainfall typically causes severe fading events in these channels, as seen in Figures 9–14, and the signal envelope received reduces faster than during stratiform rainfall. The resulting distortion effects on the PDP of the propagating signal due to the rain are presented side by side to further visualize the magnitude of the fade caused by the existence of rain along the transmission link during signal propagation across the selected frequencies. Taking a typical scenario of 60 GHz frequency (Figures 11 and 12), the overall received signal power during the stratiform rain is about -45.6 and -88.2 dBm, respectively, at the directional and omnidirectional antenna conditions (Figures 11a and 11b). This, as compared with the -55.7 and -93.3 dBm received power during the convective rain for both directional and omnidirectional antennas, respectively (Figures 12a and 12b), shows the magnitude of the effect of rainfall rate on propagated signals. Notably, the NYUSIM algorithm takes into account the specific attenuation coefficient due to rain as presented in prominent models like the ITU-R P.838-3, which takes into account the frequency and rain rate. Therefore, the resulting signal fade observed through comparison between the received power at each rain type is reliable enough to hypothesize the performance of the proposed channels at these conditions.
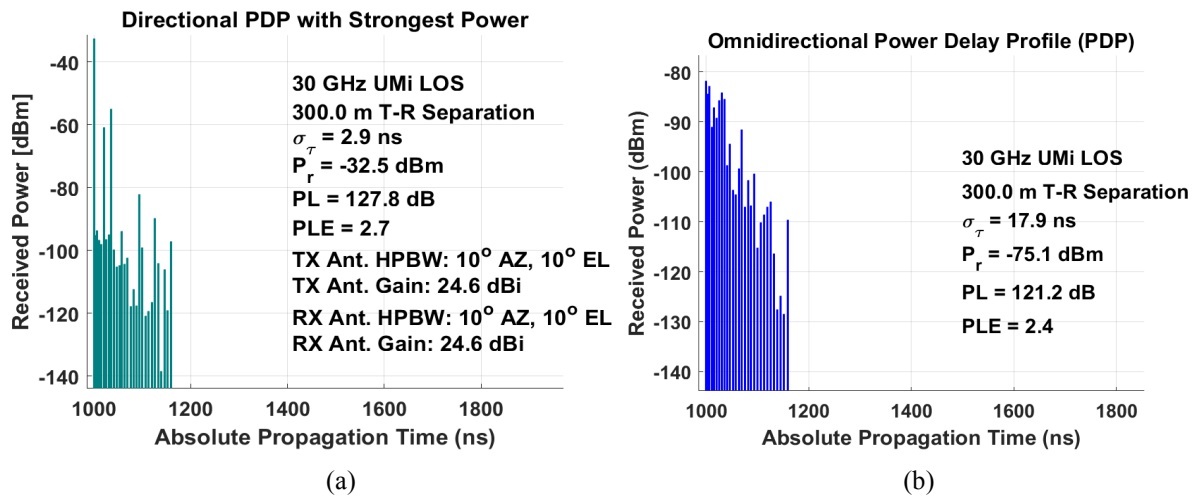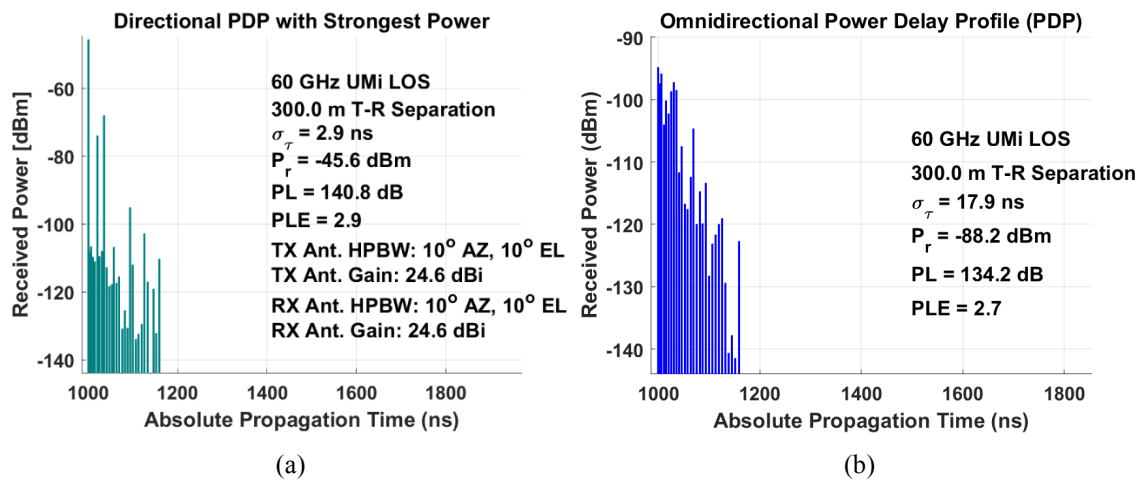

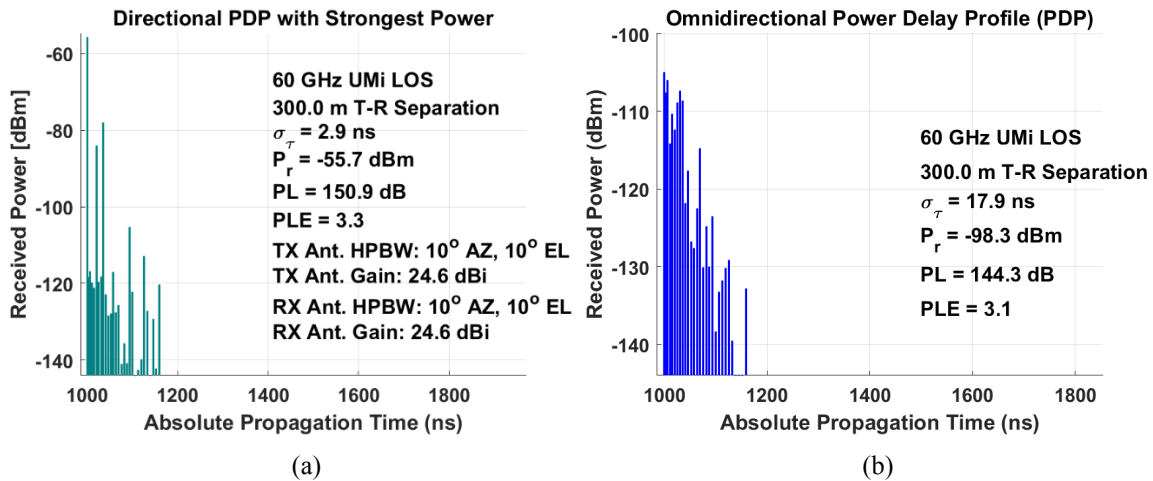**Figure 9.** PDP during Stratiform rain using (a) Oriented antenna (b) Multi-directional antenna
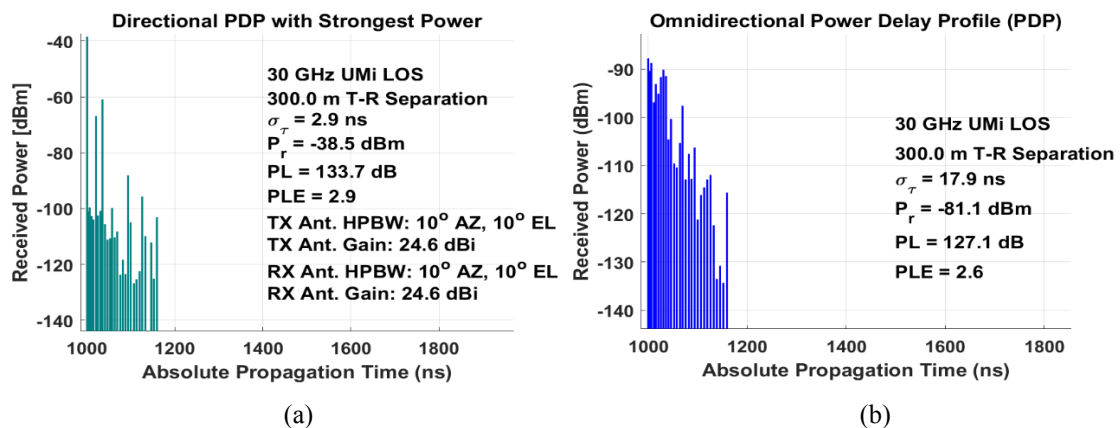
Figure 10. PDP during Convective rain using (a) Oriented antenna (b) Multi-directional antenna

The overall channel performance observed across the stratiform rain types shows more appreciable performance as compared with the convective (Figures 9–14). It is worth mentioning that the NYUSIM uses a method that searches for the pointing angle with the highest received power among all available pointing angles to identify the channel performance observed in the directional PDP. This highlights the fact that in order to compensate for the increased free-space loss associated with mmwave propagation frequencies, especially for higher frequency bands, the use of directional antennas and antenna arrays is crucial in practical mmwave communication systems. The effect of the gaseous attenuation associated with the 60 GHz (Figures 11 and 12) frequency can be observed for both directional and omnidirectional scenarios in terms of the received power and path loss ratio when compared with 100 GHz (Figures 13 and 14). Hence, much higher transmission power is recommended at this frequency and slightly above. These findings provide valuable insights into the behavior of mm-wave communication systems during different types of rainfall, which can be useful in optimizing the design and performance of mm-wave wireless systems under various weather conditions.
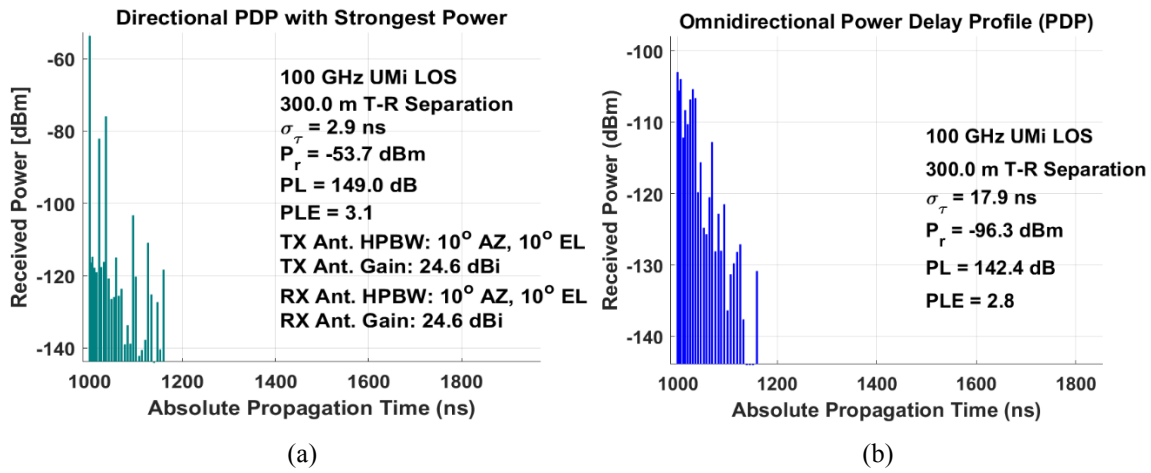

(a)   (b)

Figure 11. PDP during Stratiform rain using (a) Oriented antenna (b) Multi-directional antenna

(a)   (b)

Figure 12. PDP during Convective rain using (a) Oriented antenna (b) Multi-directional antenna
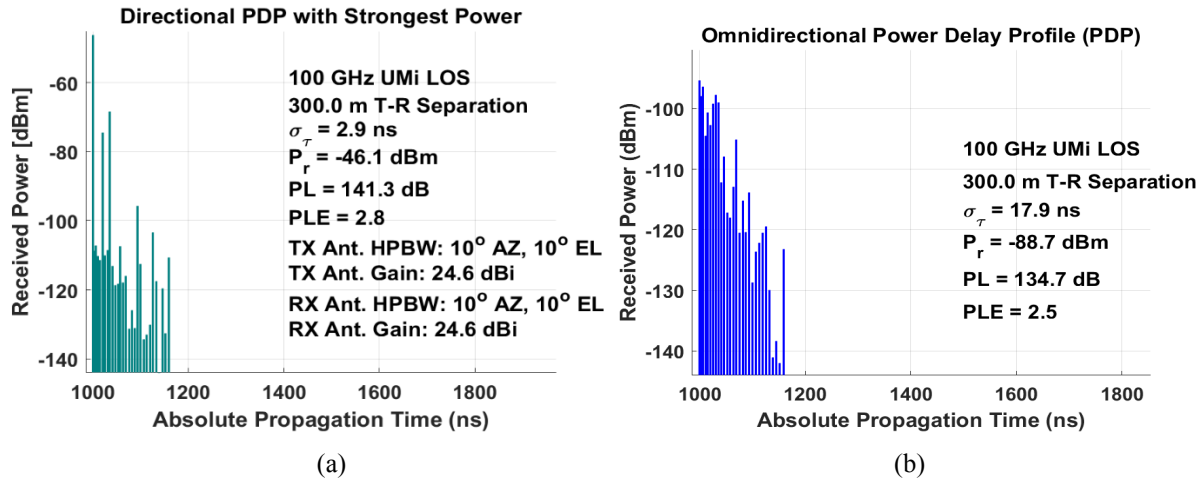
Figure 13. PDP during Stratiform rain using (a) Oriented antenna (b) Multi-directional antenna

Figure 14. PDP during Convective rain using (a) Oriented antenna (b) Multi-directional antenna

3.5 Assessment of Channel Performance at the Selected Frequencies

The overall system performance of the proposed channel model for wireless communication has been extracted from the simulator's CIRs and presented in terms of the essential LSPs over the selected frequency range. Details of the other channel parameters are discussed in this section.

3.5.1 Received Power and Fade Margin under Different Rain Types

As presented in Equ. (4) the Fade margin is the variation between the power received in dBm and the threshold of the sensitivity of the receiver. According to Ref. [27], sensitivity of the receiver can be expressed as:

$$\text{Sensitivity of the receiver (dBm)} = \text{NF} + \text{KTB noise} + \text{RF}$$

$$+ \text{path loss SNR} - \text{efficiency of the antenna} + \sum \text{coupling noise}$$

(8)

where T denotes the temperature in Kelvin, K is the Boltzmann's constant, and B represents the channel bandwidth. The RF path loss is the reduction in signal power that occurs between the modem input and antenna port of a mobile phone. The terms NF and SNR denote the noise figure and signal-to-noise ratio of radio frequency parameters, such as a power amplifier module and a phone transceiver, respectively. The sum of coupling noise can also influence the receiver's sensitivity. In this study, we adopt a receiver threshold of -108 dBm for the 959.8 MHz Extended Global System for Mobile (EGSM) band, as suggested by [31]. The selection of this threshold is informed by industry standards, such as ITU-R Recommendation P.1411-6, which provides valuable insights into the design and operation of terrestrial radio interfaces, including considerations for

receiver sensitivity and fade margins. Although the precise value is not explicitly stated in the recommendation, it offers pertinent information for defining receiver sensitivity thresholds in ITU-R (ITU-R P.1411-6). By incorporating factors such as equipment specifications, local climatic conditions, and desired reliability, the chosen threshold ensures robust signal reception in challenging tropical environments.

As presented in Figures 15 and 16, the power received and the fade margin for the channel impulse response shows the channel propagation characteristics and the resulting fade effects on the system. Generally, there is a higher fade and reduced level of received power for convective rain as compared to stratiform rain due to the difference in the rain intensity. This is evident from the variation across the frequency threshold of 30-100 GHz as presented in Figures 15 and 16. The variations across the frequency threshold should be taken into account when considering wireless propagation in tropical regions with different rain characteristics, particularly for channel propagation that utilizes the extremely high frequency (EHF) band. Additionally, the result further implies that more power is required to propagate signals at higher frequencies. As presented in Figure 15, the power received decreases as the frequency increases, while the fade margin reduces as the frequency increases (Figure 16). It is crucial that the link budget and analysis prioritize limiting the potential effects of rain attenuation since the wave propagation at the mmWave frequency for 5G and future wireless networks is highly susceptible to distortion and slight interference, whereby the propagation system is highly distorted.
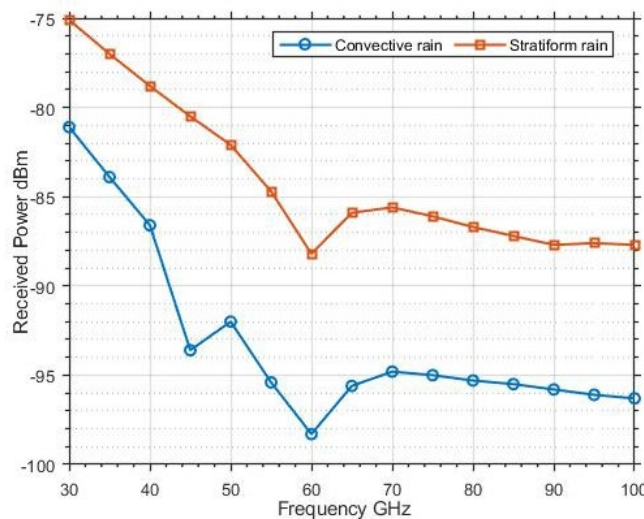
**Figure 15.** Variation of the received power (dBm) at a different frequency
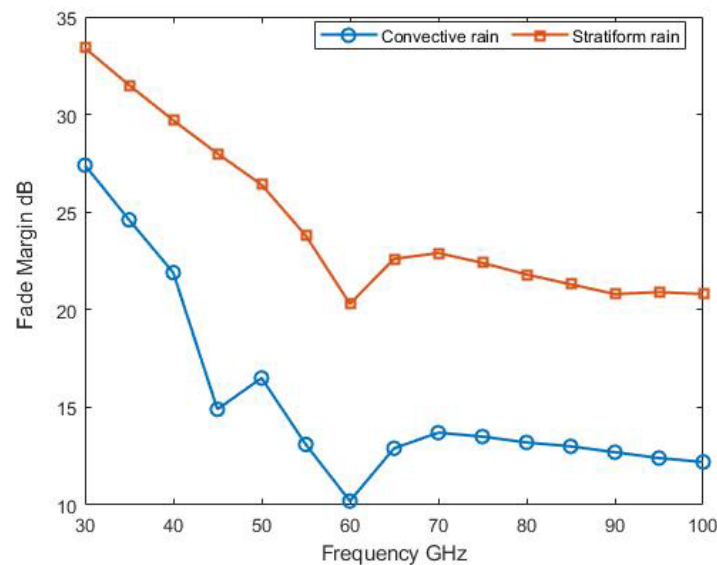
**Figure 16.** Variation of the fade margin at different frequencies

Additionally, the effect of the presence of certain gaseous molecules across the terrestrial link is observed in the received power, and the associated fade margin is indicated in Figures 15 and 16, respectively. Most importantly, the gaseous attenuation which occurs near the 60 GHz frequency i.e., 57-60 window GHz range is responsible for additional signal distortion which is shown by the rapid crests and troughs across the presented trends. This effect is also notable in Figures 17 and 18 which depict the path loss at each rainfall type in comparison with the ITU-R standard for the region [32]. This absorption results in lesser received power, more fade margin, and greater path loss in the two scenarios at the specified window range. The implication is that at such frequencies window, in addition to the increase in the path loss, there exists additional attenuation due to the gaseous effect, which may further deteriorate signal reception in the region.

3.5.2 Path loss Experienced Under Different Rain Types

The path loss distribution across the 30-100 GHz frequency for the proposed channel is presented in relation to the ITU recommendation ITU-R P.676-3 (2016) for the gaseous attenuation profile across the terrestrial link, and it is observed that both rain types exhibit the similar behavior when increasing the frequency as presented in Figures 17 and 18 for the 0.01% and 0.1% unavailability of signal respectively. However, a much higher path loss is recorded for the convective rain scenario due to a higher rain rate of 140 mm/hr when compared to the 40 mm/hr. The effect of the presence of the gaseous molecules across this propagation link is also visualized through the crests and troughs on the plots. The comparison as presented, also shows conformity in the proposed channel behavior and the standard proposition of the ITU-R. Generally, the findings will provide information for the system engineers to identify appropriate channels and frequencies for the deployment of 5G and other future wireless communication networks operating in the mmWave spectrum specifically for the studied region.
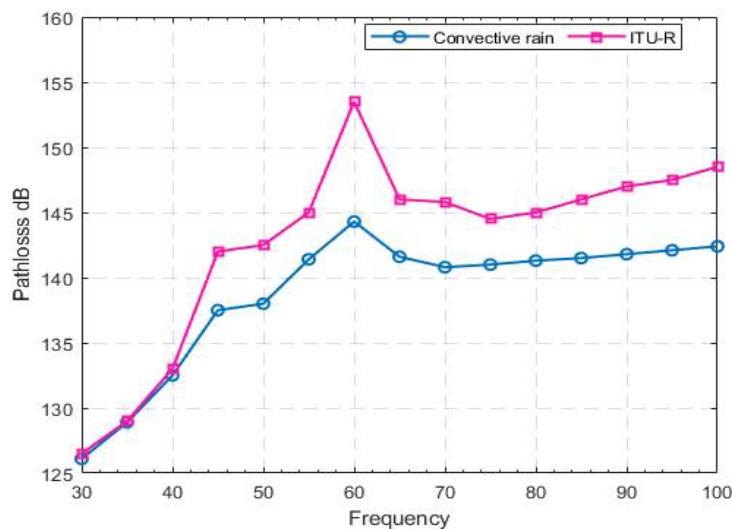
Figure 17. Path loss at 0.01% unavailability and ITU-R from 30-100 GHz
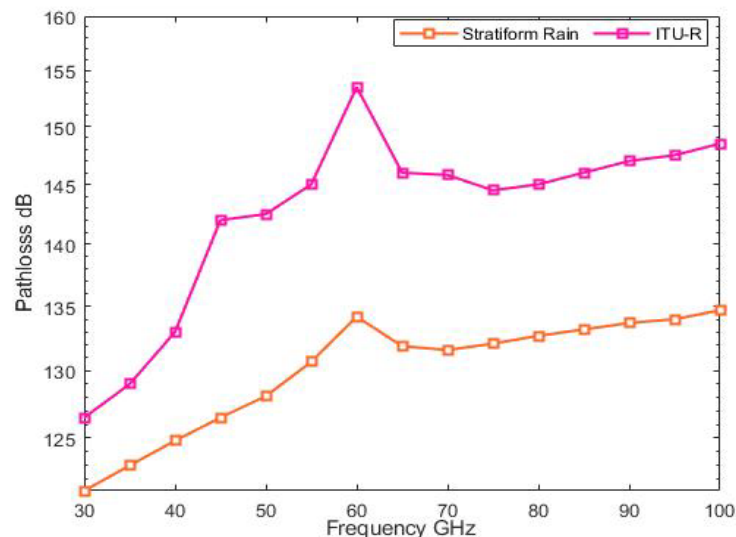
Figure 18. Path loss at 0.10% unavailability and ITU-R from 30 -100 GHz

4. CONCLUSION

This work has been based on the influence of rain on channel propagation characteristics in a tropical region. A comprehensive statistical analysis of the transmission of some mmWave frequency scenarios for the 5G deployment and future network platforms was carried out by examining the influence of rain rate variation, which is an important environmental constraint, especially in tropical regions, taking the frequency 30-100 GHz for urban microcell. The simulation was based on the NYUSIM model and several CIRs indicating the region's overall channel propagation behaviors. Generally, the result will be good for region-based 5G and future wireless connection network deployment. Additional mitigation measures are recommended for the frequency window of 57–60 GHz due to the gaseous attenuation at such frequencies.

REFERENCES

[1] Budalal AA, Rafiqul IM, Habaebi MH, Rahman TA. The effects of rain fade on millimetre wave channel in tropical climate. Bulletin of Electrical Engineering and Informatics. 2019;8(2):653-64.

[2] Budalal AA, Shayea I, Islam MR, Azmi MH, Mohamad H, Saad SA, et al. Millimetre-wave propagation channel based on NYUSIM channel model with consideration of rain fade in tropical climates. IEEE Access. 2021;10:1990-2005.

[3] Ju S, Sun S, & Rappaport T.S. NYUSIM User Manual. 2022. https://wireless.engineering.nyu.edu/nyusim/

[4] Philip AS, James JE, Antony J, Varghese JA, Sreenath M. Millimeter Wave Communications For 5g: Theory And Applications. 2020; 7(5).

[5] Alozie E, Abdulkarim A, Abdullahi I, Usman AD, Faruk N, Olayinka I-FY, et al. A review on rain signal attenuation modeling, analysis and validation techniques: Advances, challenges and future direction. Sustainability. 2022;14(18):11744.

[6] Al-Samman AM, Azmi MH, Al-Gumaei YA, Al-Hadhrami T, Abd. Rahman T, Fazea Y, et al. Millimeter wave propagation measurements and characteristics for 5G system. Applied Sciences. 2020;10(1):335.

[7] Shayea I, Abd. Rahman T, Hadri Azmi M, Arsad A. Rain attenuation of millimetre wave above 10 GHz for terrestrial links in tropical regions. Transactions on emerging telecommunications technologies. 2018;29(8):e3450.

[8] Rappaport TS, Sun S, Mayzus R, Zhao H, Azar Y, Wang K, et al. Millimeter wave mobile communications for 5G cellular: It will work! IEEE access. 2013;1:335-49.

[9] Ojo JS, Ajewole MO, Sarkar SK. Rain rate and rain attenuation prediction for satellite communication in Ku and Ka bands over Nigeria. Progress In Electromagnetics Research B. 2008;5:207-23.

[10] Hilt A. Availability and fade margin calculations for 5G microwave and millimeter-wave anyhaul links. Applied Sciences. 2019;9(23):5240.

[11] Budalal AA, Islam MR, Habaebi MH, Rahman TA, editors. Millimeter wave channel modeling–present development and challenges in tropical areas. 2018 7th International Conference on Computer and Communication Engineering (ICCCE); 2018: IEEE.

[12] Yun Z, Iskander MF. Ray tracing for radio propagation modeling: Principles and applications. IEEE access. 2015;3:1089-100.

[13] Nandi D, Maitra A. Study of rain attenuation effects for 5G Mm-wave cellular communication in tropical location. IET Microwaves, Antennas & Propagation. 2018;12(9):1504-7.

[14] Sun S, Rappaport TS, Shafi M, Tang P, Zhang J, Smith PJ. Propagation models and performance evaluation for 5G millimeter-wave bands. IEEE Transactions on Vehicular Technology. 2018;67(9):8422-39.

[15] Haneda K, Zhang J, Tan L, Liu G, Zheng Y, Asplund H, et al., editors. 5G 3GPP-like channel models for outdoor urban microcellular and macrocellular environments. 2016 IEEE 83rd vehicular technology conference (VTC spring); 2016: IEEE.

[16] Abbas T, Qamar F, Ahmed I, Dimyati K, Majed MB, editors. Propagation channel characterization for 28 and 73 GHz millimeter-wave 5G frequency band. 2017 IEEE 15th student conference on research and development (SCOReD); 2017: IEEE.

[17] Majed MB, Rahman TA, Aziz OA. Propagation path loss modeling and outdoor coverage measurements review in millimeter wave bands for 5G cellular communications. International Journal of Electrical and Computer Engineering. 2018;8(4):2254.

[18] Zaman K, Mowla MM, editors. A millimeter wave channel modeling with spatial consistency in 5G systems. 2020 IEEE region 10 symposium (TENSYMP); 2020: IEEE.

[19] Zekri AB, Ajgou R, Meftah E-H. Effect of Spatial Consistency Parameters on 5G Millimeter Wave Channel Characteristics. Progress In Electromagnetics Research B. 2021;93:67-85.

[20] Rahayu I, Firdausi A. 5G Channel Model for Frequencies 28 GHz, 73 GHz and 4 GHz with Influence of Temperature in Bandung. Jurnal Teknologi Elektro. 2022;13(02).

[21] Ram N, Gao H, Qin H, Oo MT, Htun YT, editors. Statistical channel modelling of millimetre waves at 28 GHz and 73 GHz frequency signals using MIMO antennas. Journal of Physics: Conference Series; 2021: IOP Publishing.

[22] Shafi M, Zhang J, Tataria H, Molisch AF, Sun S, Rappaport TS, et al. Microwave vs. millimeter-wave propagation channels: Key differences and impact on 5G cellular systems. IEEE Communications Magazine. 2018;56(12):14-20.

[23] Rappaport TS, MacCartney GR, Samimi MK, Sun S. Wideband millimeter-wave propagation measurements and channel models for future wireless communication system design. IEEE transactions on Communications. 2015;63(9):3029-56.

[24] Kim J, Yang K, Kim J, Kim Y, Lee S. Methodology for RF receiver sensitivity analysis using electromagnetic field map. Electronics Letters. 2014;50(23):1753-5.

[25] Wu T, Rappaport TS, Collins CM. Safe for generations to come: Considerations of safety for millimeter waves in wireless communications. IEEE microwave magazine. 2015;16(2):65-84.

[26] Ojo JS, Ijomah CK, Akinpelu SB. Artificial neural networks for earth-space link applications: A prediction approach and inter-comparison of rain-influenced attenuation models. Int J Intell Syst Appl(IJISA). 2022;14(5):47-58.

[27] Abdulwahid MM, Al-Ani OAS, Mosleh MF, Abd-Alhameed RA, editors. Investigation of millimeter-wave indoor propagation at different frequencies. 2019 4th Scientific International Conference Najaf (SICN); 2019: IEEE.

[28] Adaramola MS. Estimating global solar radiation using common meteorological data in Akure, Nigeria. Renewable Energy. 2012;47:38-44.

[29] Salvi LS, Jadhav A. Annual Rainfall Prediction of Maharashtra State Using Multiple Regression. Intelligent Computing and Networking: Proceedings of IC-ICN 2022: Springer; 2023. p. 179-90.

[30] Matricciani E, editor Global formulation of the Synthetic Storm Technique to calculate rain attenuation only from rain rate probability distributions. 2008 IEEE Antennas and Propagation Society International Symposium; 2008: IEEE.

[31] Liu Z, Li F, Qi Y, Chen J, editors. An effective receiver sensitivity measurement. 2015 IEEE Symposium on Electromagnetic Compatibility and Signal Integrity; 2015: IEEE.

[32] Makarov DS, Tretyakov MY, Rosenkranz PW. Revision of the 60-GHz atmospheric oxygen absorption band models for practical use. Journal of Quantitative Spectroscopy and Radiative Transfer. 2020; 243:106798.

[33] Budalal AA, Islam MR. Path loss models for outdoor environment—with a focus on rain attenuation impact on short-range millimeter-wave links. e-Prime-Advances in Electrical Engineering, Electronics and Energy. 2023; 3:100106.